

Research Article

Magnetic Phase Separation and Magnetic Moment Alignment in Ordered Alloys $\text{Fe}_{65}\text{Al}_{35-x}\text{M}_x$ ($\text{M}_x = \text{Ga, B; } x = 0; 5 \text{ at.}\%$)

E. V. Voronina ¹, A. K. Arzhnikov,² A. I. Chumakov,³ N. I. Chistyakova,⁴ A. G. Ivanova,¹
A. V. Pyataev,¹ and A. V. Korolev⁵

¹Institute of Physics, Kazan Federal University, Kazan 420008, Russia

²Physical-Technical Institute, Ural Branch of Russian Academy of Sciences, Izhevsk 426000, Russia

³European Synchrotron Radiation Facility, 38043 Grenoble Cedex 9, France

⁴Faculty of Physics, M. V. Lomonosov Moscow State University, Moscow 119991, Russia

⁵Institute of Metal Physics, Ural Branch of Russian Academy of Sciences, Yekaterinburg 620108, Russia

Correspondence should be addressed to E. V. Voronina; evoronina2005@yandex.ru

Received 16 October 2017; Accepted 10 January 2018; Published 1 March 2018

Academic Editor: Mohindar S. Seehra

Copyright © 2018 E. V. Voronina et al. This is an open access article distributed under the Creative Commons Attribution License, which permits unrestricted use, distribution, and reproduction in any medium, provided the original work is properly cited.

The structure and the magnetic state of ordered $\text{Fe}_{65}\text{Al}_{35-x}\text{M}_x$ ($\text{M}_x = \text{Ga, B; } x = 0; 5 \text{ at.}\%$) alloys are investigated using X-ray diffraction, Mössbauer spectroscopy, and magnetic measurements. The behavior of the magnetic characteristics and Mössbauer spectra of the binary alloy $\text{Fe}_{65}\text{Al}_{35}$ and the ternary alloy with gallium addition $\text{Fe}_{65}\text{Al}_{30}\text{Ga}_5$ is explained in terms of the phase separation into two magnetic phases: a ferromagnetic one and a spin density wave. It is shown that the addition of boron to the initial binary alloy $\text{Fe}_{65}\text{Al}_{35}$ results in the ferromagnetic behavior of the ternary alloy.

1. Introduction

One of the most intriguing topics of modern solid-state physics is noncollinear disordered [1] and ordered [2–4] structures of magnetic moments. In addition to the need to understand the cause of their existence [2], they are closely related to superconductivity [2–4] and are important for spintronic applications [5]. There are different concepts of the nature of magnetic nanostructures. It is assumed that they may arise as a result of competing exchange interactions, the Fermi surface nesting, and low-lying thermal excitations. Moreover, the very identification of the structures remains a complicated problem. In neutron-diffraction studies of B2-ordered Fe-Al alloys, a correlation of the magnetic moments with a coherence length of about 5 nm was revealed [6]. The observed ordering of the magnetic moments was explained in terms of the spin density wave (SDW). It was found that, at a concentration of $x = 35 \text{ at.}\%$ in $\text{Fe}_{100-x}\text{Al}_x$ alloys, the spin density wave has the largest coherence length. In a study [7] of the magnetotransport properties of quasi-ordered $\text{Fe}_{100-x}\text{Al}_x$ alloys, $x = 30\text{--}35 \text{ at.}\%$, the anomalies in the behavior of

the transverse magnetoresistance and the Hall constant were explained based on the model of an inhomogeneous magnetic structure. In this context, the quasi-ordered Fe-Al alloys with an Al content from 25 to 40 at.% are of interest as model objects for studying the origin and stabilization of magnetic inhomogeneities in structurally homogeneous magnets, in particular incommensurate long-period spin structures. It is assumed that small additions of a third element, for example, Ga or B, to the $\text{Fe}_{65}\text{Al}_{35}$ alloy will allow one to follow the changes in the magnetic state of the initial alloy and, thus, to clarify the peculiarities of its magnetic microstructure.

The aim of this work is to study the magnetic state of ternary quasi-ordered $\text{Fe}_{65}\text{Al}_{35-x}\text{M}_x$ ($\text{M}_x = \text{Ga, B; } x = 5 \text{ at.}\%$) alloys based on an analysis of the structure, Mössbauer and magnetometric data, and their comparison with the results of analogous studies of the $\text{Fe}_{65}\text{Al}_{35}$ alloy.

2. Experimental

The binary and ternary quasi-ordered alloys $\text{Fe}_{65}\text{Al}_{35}$ and $\text{Fe}_{65}\text{Al}_{35-x}\text{M}_x$ ($\text{M}_x = \text{Ga, B; } x = 5 \text{ at.}\%$) were obtained by heat

treatment of disordered nanocrystalline alloys synthesized by mechanochemistry. The alloys from the original powders (99.98% Fe and 99.99% Al) and a Ga or B (99.98%) additive in the appropriate weight ratio were synthesized in a FRITSCHE P-7 planetary ball mill with vials and balls of hardened steel in an Ar atmosphere for 16 hours. Next the scheme and the parameters of heat treatment were selected in such a way as to ensure the structural and chemical homogeneity of the alloys and the required state of structure (a superstructure of the $B2$ or $D0_3$ type). The chemical composition of the alloys was determined by the methods of secondary ion mass spectrometry (SIMS, MC7201) and atomic emission spectrometry (SPECTROFLAME-MODULA D with inductively coupled plasma inductively coupled plasma). The results of these studies showed that the content of additives coincided with that in the initial mixture for mechanochemistry with an accuracy of 0.5 at. %.

Attestation of the structure was carried out by X-ray diffraction (XRD) at room temperature using a SMARTLAB (Rigaku) diffractometer with $\text{Cu K}\alpha$ -monochromated radiation. The phase composition of the obtained materials was determined by the Rietveld analysis of the diffraction data, using the PDXL 2 software and the ICDD (PDF-2) database. The Mössbauer spectra on the ^{57}Fe nucleus were measured at the Nuclear resonant scattering station ID18 [8] of the European Synchrotron Radiation Facility (ESRF) using a Synchrotron Mössbauer Source [9]. The measurements were carried out at a temperature of 4.2 K, both without an external magnetic field and in an applied external field $H_{\text{ext}} = 5$ T. The direction of the external magnetic field was chosen to be vertical, that is, perpendicular to the direction of the gamma radiation incident on the samples and perpendicular to the direction of the magnetic vector of almost completely ($\sim 99\%$) polarized radiation from the Synchrotron Mössbauer Source [9]. Under these conditions, the measured Mössbauer spectra should contain only the components of hyperfine transitions with a change in the quantum number of the magnetic moment projection, $\Delta m = \pm 1$, which greatly facilitates the interpretation of the results. The Mössbauer spectra were fitted using the software product SpectrRelax [10]. Magnetic measurements were performed at the Magnetometry Center of the IMF UrB RAS on a SQUID magnetometer MPMS-XL5 (Quantum Design) in external magnetic fields up to 5 T at temperatures from 5 to 400 K.

3. Results and Discussion

The X-ray-diffraction analysis data indicate that the alloys investigated are of single phase in structure and are chemically homogeneous. In the diffractograms of all samples of the $\text{Fe}_{65}\text{Al}_{35}$ and $\text{Fe}_{65}\text{Al}_{30}\text{Ga}_5$ alloys, only reflexes of the $B2$ -superstructure are present (Figure 1). No diffuse background indicating the presence of $D0_3$ -ordered regions is detected. For the $\text{Fe}_{65}\text{Al}_{35}\text{B}_5$ alloy, superstructural reflections of a $D0_3$ -type lattice are revealed. To obtain a single-phase structure of the sample $\text{Fe}_{65}\text{Al}_{35}\text{B}_5$, it was heat-treated at a relatively low temperature of 400°C . Despite the presence of superstructural (110), (200), (311) reflections on the diffractogram of this sample, all the reflections are noticeably broadened. For a

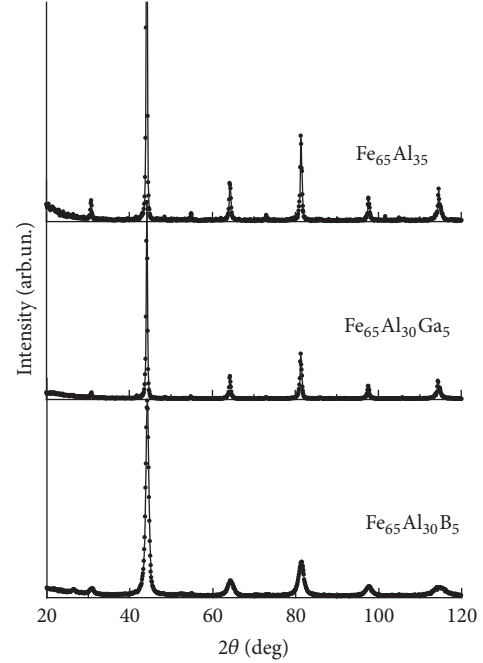


FIGURE 1: X-ray-diffraction patterns of the quasi-ordered $\text{Fe}_{65}\text{Al}_{35}$ and $\text{Fe}_{65}\text{Al}_{35-x}\text{M}_x$ ($\text{M}_x = \text{Ga}, \text{B}; x = 5$ at. %) alloys. $\text{Cu K}\alpha$ -radiation, $T = 300$ K.

sample subjected to prolonged annealing, such broadening is apparently caused by the small size of the regions of X-ray coherent scattering. This, in turn, suggests a higher degree of disordering of this sample in comparison with $\text{Fe}_{65}\text{Al}_{35}$ and $\text{Fe}_{65}\text{Al}_{30}\text{Ga}_5$. An increase of 0.1% in the bcc lattice parameter of the ternary alloy with a 5 at. % Ga additive is observed as compared to $\text{Fe}_{65}\text{Al}_{35}$. For the $\text{Fe}_{65}\text{Al}_{30}\text{B}_5$ alloy, the lattice parameter decreases by 0.3% (Table 1).

As seen from Figure 2, for the $\text{Fe}_{65}\text{Al}_{35}$ and $\text{Fe}_{65}\text{Al}_{30}\text{Ga}_5$ alloys, the magnetization curves do not reach saturation in external magnetic fields up to $H_{\text{ext}} = 5.0$ T. The technical saturation at $H_{\text{ext}} = 3$ T, characteristic for a ferromagnet, is observed only for the $\text{Fe}_{65}\text{Al}_{30}\text{B}_5$ alloy. Hysteresis loops are unbiased and symmetric, and the coercive force values estimated from the hysteresis loop are small (Table 1). The value of the specific saturation magnetization σ_0 was estimated by extrapolating the high-field part of the magnetization curve to $H_{\text{ext}} = 0$ (shown in Figure 2 by dashed lines). The magnetic moment per Fe atom, \overline{m}_{Fe} , calculated from σ_0 , is also given in Table 1. The results obtained agree with the magnetic measurements at $T = 4.2$ K in [11], where it was shown that the magnetization does not reach saturation in deformed $\text{Fe}_{100-x}\text{Al}_x$ alloys with $x > 40$ at. % in pulsed magnetic fields up to 15.0 T. The values of magnetization in the hysteresis loops in the ZFC and FC cycles of $\text{Fe}_{65}\text{Al}_{30}\text{Ga}_5$ coincide at the relevant temperature (5 K) and field, while the virgin magnetization curve lies well below the hysteresis loop (Figure 2, inset). The susceptibilities of the initial section of the virgin magnetization curve and of the analogous section of the hysteresis loop differ by a factor of two.

TABLE 1: Structural and magnetic parameters of quasi-ordered alloys $\text{Fe}_{65}\text{Al}_{35}$ and $\text{Fe}_{65}\text{Al}_{35-x}\text{M}_x$ ($\text{M}_x = \text{Ga}, \text{B}; x = 5 \text{ at.}\%$): the lattice type and parameter; the magnetic ordering temperature T_C ; the saturation magnetization σ_0 , in brackets—the magnetic moment per Fe atom \bar{m}_{Fe} ; the coercive force H_C ; the average HFF $\langle B_{\text{hf}} \rangle$ calculated from $p(B_{\text{hf}})$, in brackets— $\langle B_{\text{hf}} \rangle$ at $H_{\text{ext}} = 5 \text{ T}$.

Alloy	Lattice type	Lattice parameter*, nm	Temperature T_C , K	Magnetization σ_0 , $\text{A}\cdot\text{m}^2/\text{kg}$ ($\bar{m}_{\text{Fe}}, \mu_B/\text{Fe}$)	Coercive force, A/m	$\langle B_{\text{hf}} \rangle$, T
$\text{Fe}_{65}\text{Al}_{35}$	B2	0.2894	340	15 (0.3–0.4)	$5.17 \cdot 10^3$	14.0 (13.1)
$\text{Fe}_{65}\text{Al}_{30}\text{Ga}_5$	B2	0.2897	400	30 (0.7–0.8)	$5.57 \cdot 10^2$	15.5 (13.6)
$\text{Fe}_{65}\text{Al}_{30}\text{B}_5$	$D0_3$	0.5772	620	89 (2.2)	$1.03 \cdot 10^4$	19.8 (16.2)

*The error in determining the lattice parameter by X-ray diffraction: $\pm 1 \cdot 10^{-4} \text{ nm}$ for $\text{Fe}_{65}\text{Al}_{35}$ and $\text{Fe}_{65}\text{Al}_{30}\text{Ga}_5$ and $\pm 4 \cdot 10^{-4} \text{ nm}$ for $\text{Fe}_{65}\text{Al}_{30}\text{B}_5$.

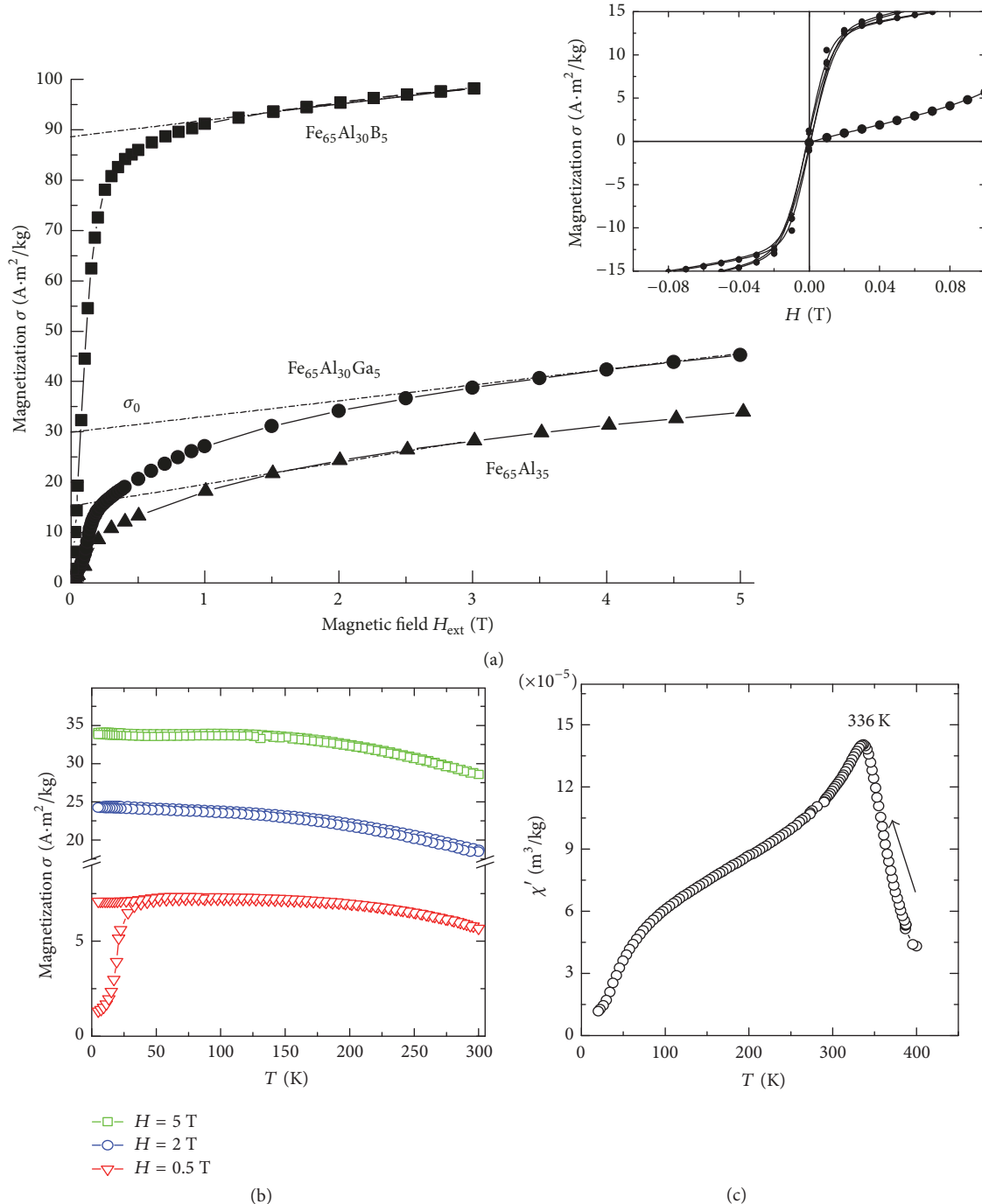


FIGURE 2: (a) Virgin magnetization curves of quasi-ordered alloys $\text{Fe}_{65}\text{Al}_{35}$ and $\text{Fe}_{65}\text{Al}_{35-x}\text{M}_x$ ($\text{M}_x = \text{Ga}, \text{B}; x = 5 \text{ at.}\%$). The inset: the virgin magnetization curve and the hysteresis loop for the alloy $\text{Fe}_{65}\text{Al}_{30}\text{Ga}_5$; (b) ZFC and FC cycles for $\text{Fe}_{65}\text{Al}_{30}\text{Ga}_5$ alloy at $H_{\text{ext}} = 0.5, 2, 5 \text{ T}$; (c) the real part of AC susceptibility of the alloy $\text{Fe}_{65}\text{Al}_{35}$.

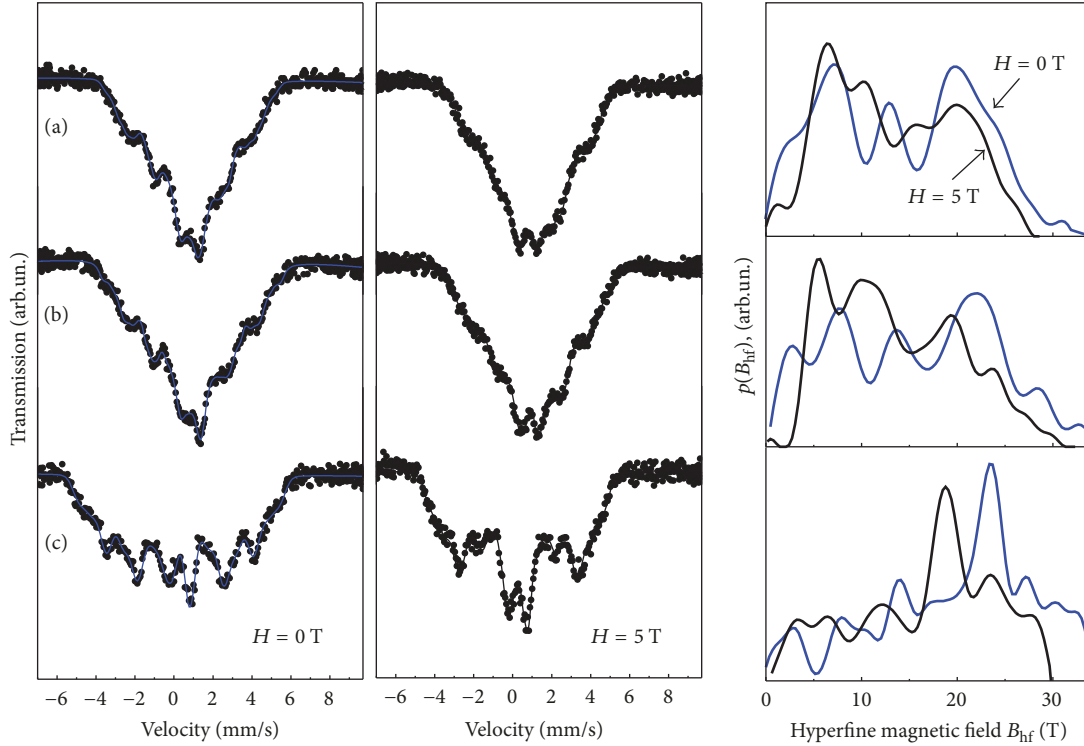


FIGURE 3: Mössbauer spectra and HFF distributions for the alloys: (a) $\text{Fe}_{65}\text{Al}_{35}$, (b) $\text{Fe}_{65}\text{Al}_{30}\text{Ga}_5$, (c) and $\text{Fe}_{65}\text{Al}_{30}\text{B}_5$. Mössbauer spectra were measured without external field (left column, dotted line) in an applied external magnetic field $H_{\text{ext}} = 5$ T (central column, dotted line). Calculated for HFF distributions $p(B_{\text{hf}})$, Mössbauer spectra are represented by solid lines. For HFF distributions $p(B_{\text{hf}})$, blue curve in the right column corresponds to Mössbauer spectra measured without external field; black curve in the right column corresponds to the spectra measured in an external magnetic field $H_{\text{ext}} = 5$ T.

The temperature magnetization curves $\sigma(T)$, measured under cooling in a magnetic field and in a zero magnetic field (FC and ZFC), show the presence of hysteresis in small fields (0.005–0.1 T). At higher values of the external field, the hysteresis disappears. A comparison of the $\sigma(H)$ values for the hysteresis loop and the ZFC and FC cycles shows that they are close. Apparently, the observed hysteresis is magnetic rather than thermomagnetic in character. The temperature dependence of the magnetic susceptibility of the investigated alloys has the form characteristic for an antiferromagnet [12] and makes it possible to estimate the temperature of transition to the paramagnetic state: for the $\text{Fe}_{65}\text{Al}_{30}\text{Ga}_5$ alloy, $T_C = 400$ K, which is higher compared to the binary alloy $\text{Fe}_{65}\text{Al}_{35}$ (≈ 340 K). The observed peculiarities of the field and temperature behavior of the magnetic characteristics allow us to state that in the low-temperature range the magnetic state of the alloys investigated cannot be unambiguously assigned to any of the well-known types of magnetic ordering [13].

Figure 3 presents the Mössbauer spectra measured with and without an external field and the corresponding hyperfine magnetic field (HFF) distributions $p(B_{\text{hf}})$ (blue and black lines). It is obvious that the addition of gallium to the $\text{Fe}_{65}\text{Al}_{35}$ alloy leads to an increase in the “integral” average magnetic characteristics: magnetization and the mean HFF. The introduction of a 5 at.% boron additive causes a sharp

increase in the magnetization (by a factor of three) and the mean HFF (by 5.8 T).

According to the magnetic measurements, the magnetic moment for the $\text{Fe}_{65}\text{Al}_{35}$ alloy is 0.3–0.4 μ_B/Fe atom (Table 1). If this alloy is considered to be a single-phase ferromagnet, then based on the mean HFF value of 14.0 T and using the known coefficient $\langle B_{\text{hf}} \rangle / \bar{m}_{\text{Fe}}: 11.0 \div 12.0 \text{ T}/\mu_B$ [14, 15] for ferromagnetic systems of iron with sp -elements, one can estimate the magnetic moment per Fe atom in the alloy, \bar{m}_{Fe} . Thus, the magnetic moment \bar{m}_{Fe} calculated from the Mössbauer measurements is 1.1–1.2 μ_B/Fe for $\text{Fe}_{65}\text{Al}_{35}$ and 1.3 μ_B/Fe for $\text{Fe}_{65}\text{Al}_{30}\text{Ga}_5$, which is, respectively, 3 and 1.5 times larger than the values obtained from the magnetic measurements.

The resolved hyperfine structure in the Mössbauer spectra of Fe alloys with an Al content above 25 at.% is lacking. In a series of studies, this was considered as the result of an increase in the number of possible local environments of Fe atoms in superstructures of nonstoichiometric composition or a manifestation of the itinerant magnetism. Mössbauer, magnetometric, and neutron diffraction studies [11, 16–19] led to the assumption of the existence of clusters or groups of magnetic moments forming magnetic microinhomogeneities in ordered Fe-Al alloys. However, these revealed magnetic inhomogeneities differ significantly in the size: from one or

several unit cells [11] to 2–4 nm [16]. In addition, in a number of papers, the idea of the existence of oppositely oriented magnetic moments in ordered Fe-Al alloys was advanced, which was explained, for example, by antiferromagnetic indirect exchange interaction between the Fe atoms separated by an Al atom [17, 20] or negative exchange interaction due to the RKKY interaction. Theoretical calculations of the electronic structure and local magnetic moments of ordered Fe-Al alloys (29–44 at.% Al) within the density functional theory [21] have shown a possibility for the existence in these alloys of three types of magnetic ordering with a small energy difference between the states: the collinear local antiferromagnetic, ferromagnetic alignment, and the spiral spin density wave. The estimated difference in energy between these states did not exceed 7 mRy/cell. In the ground state, the most energetically preferable are the spin density wave and the local antiferromagnetic state. However, the energy of the ferromagnetic state is so close that, under external influences or with changes in the boundary conditions and lattice parameters, the probability that this state will arise is high. This suggests the possibility of magnetic phase separation in such systems. In addition, the authors of the work noted the dependence of the magnetic moment magnitude and direction on the number of Al atoms in the nearest environment of the Fe atom.

Neutron diffraction studies of the B2-ordered Fe-Al alloys with Al concentrations of 34–43 at.% confirmed the existence of spatial correlations between the magnetic moments with a coherence length of about 5 nm, which were interpreted in terms of spin density wave.

When studying the transverse magnetoresistance and the Hall effect in the ordered alloys $\text{Fe}_{100-x}\text{Al}_x$, $x = 30\text{--}35$ at.%, the authors of [7] revealed anomalies of the magnetotransport properties explained in the context of the spatially inhomogeneous magnetic structure model.

The spectra were fitted in a discrete representation with the number of sextets equal to the number of centers detected in the HFF distribution $p(B_{\text{hf}})$, with each center being assigned to the nucleus of the ^{57}Fe atom in a certain local environment. It was also assumed that the parameters of the local atomic environment (the HFF of ^{57}Fe and the configuration probabilities) are close to those of the corresponding local configurations for ordered Fe-Al alloys [22]. However, no satisfactory description of the Mössbauer spectra was obtained within the model of local atomic environments.

It was expected that low-temperature Mössbauer measurements in an external magnetic field would provide additional information for the selection of an adequate model of Mössbauer spectra. It is known that, in the spectra of a polycrystalline ferromagnetic material with $m_{\text{Fe}} \uparrow \downarrow B_{\text{hf}}$ in a magnetic field whose direction is parallel to that of the magnetic vector of incident radiation, which was realized in this study, two changes are observed: the ratio of the elementary sextet line intensities changes from 3:2:1 to 3:0:1, and $p(B_{\text{hf}})$ is shifted into the region of smaller values by the amount of the applied magnetic field. For the samples under investigation, a similar behavior (of the ferromagnetic type) occurs only for the $\text{Fe}_{65}\text{Al}_{30}\text{B}_5$ alloy, in the spectrum of which an apparent decrease in the intensity of the second

and fifth lines of the sextet is observed, and the mean HFF decreases by 3.6 T (Figure 4). For the $\text{Fe}_{65}\text{Al}_{35}$ and $\text{Fe}_{65}\text{Al}_{30}\text{Ga}_5$ alloys, an application of an external magnetic field of 5 T leads to a decrease in the mean value of HFF by 0.9 T and 1.9 T, respectively. The changes observed in $p(B_{\text{hf}})$ point to inhomogeneous magnetic structure of the $\text{Fe}_{65}\text{Al}_{35}$ and $\text{Fe}_{65}\text{Al}_{30}\text{Ga}_5$ alloys. Components are detected, the effective HFF of which decreases when an external field is applied. These components correspond to the Fe atoms, the orientation of the magnetic moments of which coincides with the direction of the applied magnetic field. The values of the effective HFF on the nuclei of such atoms lie in the range from 12.0–15.0 to 33.0 T. A comparison of the HFF distributions (Figure 3) shows that the spectra contain also a component whose behavior is nontypical for the ferromagnetic alignment of magnetic moments. This component is characterized by the HFF values in the range from 0 to 15.0–17.5 T. For the $\text{Fe}_{65}\text{Al}_{30}\text{B}_5$ alloy, a comparison of the Mössbauer spectra and $p(B_{\text{hf}})$, measured in an external magnetic field and without it, shows that the magnetic state of this alloy is of the ferromagnetic type.

Based on the above-mentioned experimental and theoretical literature data and the results of measurements carried out in this work, the following model of the magnetic microstructure of the $\text{Fe}_{65}\text{Al}_{35}$ and $\text{Fe}_{65}\text{Al}_{30}\text{Ga}_5$ alloys is proposed. The spectrum is presented as follows:

(1) There is a contribution from resonant atoms in the ferromagnetic phase, for which the values of the local HFF depend on the local environment and can be represented by the local HFF distribution $p(B_{\text{hf}})$.

(2) There is a contribution from resonant atoms for which the values of the local HFF (and, correspondingly, the magnetic moments) vary from site to site of the crystal lattice proportionally to the spin density wave.

There are a lot of examples of estimating the Mössbauer experiment data in the SDW model [23, 24]. The spin density wave is a stationary periodic field of electron spin density in the crystal lattice. It is assumed that the HFF on the nucleus of a resonant atom in the mid position in the crystal lattice is proportional to the SDW amplitude in this position. We assume the SDW to be collinear and antiferromagnetic. In addition, the SDW is assumed to have a symmetry similar to that found earlier, for example, in chromium [25]. The SDW can be described by a series of odd harmonics, and the SDW amplitude (B_{hf}) can be expressed in the form [26]

$$B_{\text{hf}}(qx) = \sum_{n=1}^N b_{2n-1} \sin[(2n-1)qx], \quad (1)$$

where the symbol b_{2n-1} denotes the amplitude of the successive harmonics, the variable q is the wave number of the SDW, and the symbol x designates the relative position of the resonance nucleus along the stationary SDW propagation direction. The index N numbers the highest necessary harmonic. By virtue of the SDW periodicity, the argument qx satisfies the following condition: $0 \leq qx \leq 2\pi$. The average amplitude of the SDW, $\langle B_{\text{hf}} \rangle$, described by expression (1), is zero. The amplitude of the first harmonic b_1 is positive by definition, since the absolute phase shift between the

TABLE 2: The results of the spectra fitting for the $\text{Fe}_{65}\text{Al}_{35}$ and $\text{Fe}_{65}\text{Al}_{30}\text{Ga}_5$ alloys without external field and in an applied magnetic field $H_{\text{ext}} = 5$ T: the fraction of the ferromagnetic type phase S_F , the SDW fraction S_{SDW} , the average HFF of the ferromagnetic subsystem $\langle B_{\text{hf}}(F) \rangle$, and the harmonic amplitudes b_{2n+1} , describing the SDW by formula (1).

Alloy		S_F , %	S_{SDW} , %	$\langle B_{\text{hf}}(F) \rangle$, T	b_1	b_3	b_5	b_7	b_9
$\text{Fe}_{65}\text{Al}_{35}$	$H = 0$ T	20–30	80–70	23.0	183.8	–24.0	15.7	0.0	0.0
$\text{Fe}_{65}\text{Al}_{30}\text{Ga}_5$	$H = 0$ T	45–55	55–45	23.3	137.8	–10.1	9.7	0.66	0.0
$\text{Fe}_{65}\text{Al}_{35}$	$H = 5$ T	47	53	17.8	138.2	18.3	13.9	10.4	–17.4
$\text{Fe}_{65}\text{Al}_{30}\text{Ga}_5$	$H = 5$ T	60	40	17.6	128.5	11.9	18.8	3.9	–2.6

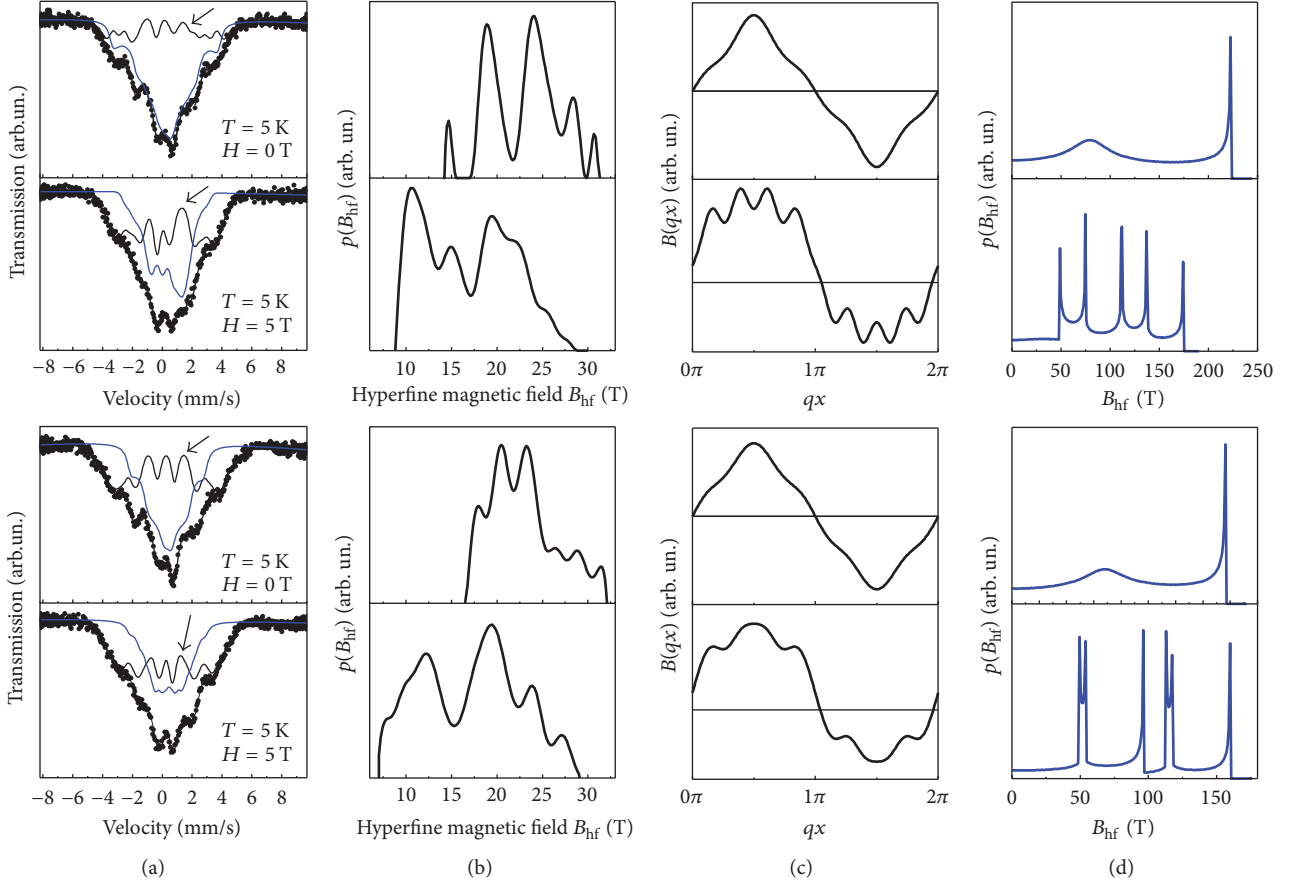


FIGURE 4: (a) Mössbauer spectra measured without external field and in an applied external magnetic field $H_{\text{ext}} = 5$ T for the alloys $\text{Fe}_{65}\text{Al}_{35}$ and $\text{Fe}_{65}\text{Al}_{30}\text{Ga}_5$. The spectrum components corresponding to the subsystems of the ferromagnetic type (black colour, shown by the arrow) and of the SDW (blue color) are presented, as well as the resulting spectrum envelope; (b) the HFF distributions of the ferromagnetic-type component; (c) the shape of the spin density wave; (d) the HFF distribution resulting from the SDW shape.

SDW and the crystal lattice generally is not observed in the framework of the method used. The amplitudes of the subsequent harmonics in the experimental spectrum processing are variable parameters. The electric quadrupole interaction is considered as a perturbation of the first order of smallness, because it is small compared to the magnetic interaction for all the cases under consideration. The results of MS fitting in the framework of this model are presented in Table 2.

The major contribution to the MS of the $\text{Fe}_{65}\text{Al}_{35}$ alloy ($H_{\text{ext}} = 0$ T) comes from a long-period magnetic structure of the SDW type, whose fraction is no less than 70%. For the

alloy with gallium addition, this contribution is much smaller but not less than that of the ferromagnetic-type phase. As seen from Figure 4, in these alloys, the SDW has a “triangular” shape, for which the distribution $p(B_{\text{hf}})$ is fairly uniform, “flat” [26]. In the spectra measured with $H_{\text{ext}} = 5$ T, the shape of the SDW changes to “rectangular”; higher-order harmonics appear. The distribution $p(B_{\text{hf}})$ for the SDW of this form is a Dirac delta function.

In the adopted SDW approximation, we assume a zero contribution to the magnetization from atoms with the SDW-generating magnetic moments. With consideration for the fraction and the average HFF $\langle B_{\text{hf}}(F) \rangle$ of the ferromagnetic

phase, the magnetic moment \overline{m} is estimated to be $0.42 \mu_B/\text{Fe}$ for $\text{Fe}_{65}\text{Al}_{35}$ and $0.8 \mu_B/\text{Fe}$ for $\text{Fe}_{65}\text{Al}_{30}\text{Ga}_5$. It should be noted that in the ferromagnetic phase region one cannot exclude the presence of atoms with magnetic moments, the direction of which is opposite to the total magnetization. The magnitude and direction of these magnetic moments are determined by the characteristics of the local environment of the atom [22]. As the proportion of such atoms is small, the rather rough two-phase approximation makes it possible to reach a satisfactory agreement with the magnetometry data.

When an external magnetic field is applied, the average value of the HFF of the ferromagnetic subsystem is reduced by an amount approximately equal to the applied field. At the same time, due to the decrease of the SDW contribution, the fraction of the ferromagnetic subsystem increases. The observed changes in the contributions to the Mössbauer spectrum make it possible to conclude that when the investigated alloys are exposed to a magnetic field, there occurs a change in the spatial arrangement and the proportion of the two magnetic phases.

Based on the known literature data and the results of magnetometric and Mössbauer investigations in the present work, the magnetic microstructure of the $\text{Fe}_{65}\text{Al}_{35}$ and $\text{Fe}_{65}\text{Al}_{30}\text{Ga}_5$ alloys in the ground state can be qualitatively represented as a set of regions characterized by two different types of order. In the absence of an external field and at low temperatures, the region with ferromagnetically ordered moments occupies a small part of the material volume. In this region, there may chaotically occur atoms with the magnetic moments, whose direction is opposite to the total magnetization of the region. Most of the crystallite bulk is occupied by regions (or clusters) in which the spin density, the related magnetic moment, and effective HFF on the nuclei of ^{57}Fe atoms vary periodically from site to site. In such regions, covering several cells of the crystal lattice ($10 \div 15$), the arrangement of the collinear magnetic moments is described in the spin density wave representation. It is the presence of these regions that leads to the large paramagnetic contribution to the magnetic susceptibility of the material, observed at low temperatures and small external fields. First, as the external magnetic field increases, the ferromagnetic region gets magnetized. Then the magnetic moments in the SDW region change gradually their orientation to be more favorable with respect to the external magnetic field direction, and SDW region “dissolves” (becomes smaller) in the ferromagnetic region which increases in volume. That is, during the material magnetization, there occurs a change in the spatial arrangement and the proportion of the two magnetic phases in the crystal lattice, which explains the unusual behavior of the virgin magnetization curve relative to the hysteresis loop on magnetization.

In the alloy with the addition of gallium, the fraction of the SDW is noticeably smaller. As possible causes of this experimental evidence, one can mention an increase in the interatomic spacing, composition fluctuations, and/or increasing disordering, which immediately results from a chaotic substitution of Al atoms by Ga atoms in the lattice of the initial alloy. According to the conclusions of the theoretical work [21], even small perturbations of the parameters

of the nearest environment in ordered Fe-Al alloys can lead to the realization of the ferromagnetic alignment of the magnetic moments rather than the SDW.

The ferromagnetic behavior of the $\text{Fe}_{65}\text{Al}_{30}\text{B}_5$ alloy, mainly observed in magnetic and Mössbauer experiments, is most likely due to its structural state. The small size of the regions of coherent X-ray scattering, as evidenced by XRD studies, results in a high-degree disorder in the atomic arrangement of the $D0_3$ superstructure, since a large part of the atoms are located directly on or near the crystallite boundaries. In addition, according to our estimate, the size of the coherent-scattering regions for this alloy is of the same order of magnitude as the SDW coherence length in Fe-Al alloys [6]. All this in aggregate may be responsible for the ferromagnetic ordering of the magnetic moments.

4. Conclusions

In this paper, we propose an explanation of the observed behavior of the magnetic characteristics of $\text{Fe}_{65}\text{Al}_{35-x}\text{M}_x$ ($\text{M}_x = \text{Ga}, \text{B}; x = 0; 5 \text{ at.}\%$) alloys within the magnetic phase separation model, which presupposes the existence of at least two magnetic subsystems: ferromagnetic or ferrimagnetic and spin density wave. The accepted model representations make it possible to obtain a satisfactory agreement of the magnetic moment values from Mössbauer and magnetic measurements and to interpret the observed behavior of the alloys in an external magnetic field as a result of changes in the spatial arrangement and the proportions of the magnetic phases. Although the main qualitative changes in the magnetic characteristics of the $\text{Fe}_{65}\text{Al}_{35}$ and $\text{Fe}_{65}\text{Al}_{30}\text{Ga}_5$ alloys are reproducible in this representation, the chosen model requires further experimental and theoretical study of the features of long-period magnetic structures of the SDW type under the action of temperature and external magnetic field. The $\text{Fe}_{65}\text{Al}_{30}\text{B}_5$ alloy demonstrates the behavior characteristic of a ferromagnet.

Conflicts of Interest

The authors declare that there are no conflicts of interest.

Acknowledgments

The authors are grateful to the ESRF (station ID18) for the opportunity to perform the Mössbauer measurements (Grant HC-1907). This work was funded by the subsidy allocated to Kazan Federal University for the state assignment in the sphere of scientific activities (3.7352.2017/8.9).

References

- [1] M. van Schilfgaarde, I. A. Abrikosov, and B. Johansson, “Origin of the Invar effect in iron-nickel alloys,” *Nature*, vol. 400, no. 6739, pp. 46–49, 1999.
- [2] S. Mühlbauer, B. Binz, F. Jonietz et al., “Skyrmion lattice in a chiral magnet,” *Science*, vol. 323, no. 5916, pp. 915–919, 2009.
- [3] J. M. Tranquada, B. J. Sternlieb, J. D. Axe, Y. Nakamura, and S. Uchida, “Evidence for stripe correlations of spins and holes in

- copper oxide superconductors,” *Nature*, vol. 375, no. 6532, pp. 561–563, 1995.
- [4] C. de la Cruz, Q. Huang, J. W. Lynn et al., “Magnetic order close to superconductivity in the iron-based layered $\text{LaO}_{1-x}\text{F}_x\text{FeAs}$ systems,” *Nature*, vol. 453, no. 7197, pp. 899–902, 2008.
- [5] A. Manchon, N. Ryzhanova, A. Vedyayev, and B. Dieny, “Spin-dependent diffraction at ferromagnetic/spin spiral interface,” *Journal of Applied Physics*, vol. 103, no. 7, Article ID 07A721, 2008.
- [6] D. R. Noakes, A. S. Arrott, M. G. Belk et al., “Incommensurate spin density waves in iron aluminides,” *Physical Review Letters*, vol. 91, no. 21, Article ID 217201, pp. 1–4, 2003.
- [7] A. E. Elskova, N. S. Perov, V. N. Prudnikov et al., “Magnetoresistance and the hall effect of the ordered alloys $\text{Fe}_{100-x}\text{Al}_x$ ($25 < x < 35$ at. %),” *Physics of the Solid State*, vol. 50, no. 6, pp. 1071–1075, 2008.
- [8] R. Rüffer and A. I. Chumakov, “Nuclear resonance beamline at ESRF,” *Hyperfine Interactions*, vol. 97, no. 1, pp. 589–604, 1996.
- [9] V. Potapkin, A. I. Chumakov, G. V. Smirnov et al., “The ^{57}Fe synchrotron Mössbauer source at the ESRF,” *Journal of Synchrotron Radiation*, vol. 19, no. 4, pp. 559–569, 2012.
- [10] M. E. Matsnev and V. S. Rusakov, *Mössbauer Spectroscopy in Materials Science-2012: Proceedings of the International Conference MSMS-12*, vol. 1489 of *American Institute of Physics Conference Series*, 2012.
- [11] M. J. Besnus, A. Herr, and A. J. P. Meyer, “Magnetization of disordered cold-worked Fe-Al alloys up to 51 at.% Al,” *Journal of Physics F: Metal Physics*, vol. 5, no. 11, pp. 2138–2147, 1975.
- [12] E. V. Voronina, E. P. Elskov, S. K. Godovikov, A. V. Korolev, and A. E. Elskova, “Temperature and field behavior of magnetic properties of ordered alloys $\text{Fe}_{100-x}\text{Al}_x$ ($25 < x < 35$ at %),” *The Physics of Metals and Metallography*, vol. 109, no. 5, pp. 417–426, 2010.
- [13] C. M. Hurd, “Varieties of magnetic order in solids,” *Contemporary Physics*, vol. 23, no. 5, pp. 469–493, 1982.
- [14] E. P. Elskov, G. N. Konygin, E. V. Voronina et al., “YAGR-issledovaniya formirovaniya magnitnykh svoystv v neuporyadochennykh sistemakh $\text{Fe}_{100-x}\text{M}_x$ ($M = \text{Al}, \text{Si}, \text{P}$),” *Izvestiya Rossiiskoi Akademii Nauk. Seriya Fizicheskaya*, vol. 56, no. 7, pp. 119–123, 1992 (Russian).
- [15] E. P. Yelsukov, E. V. Voronina, G. N. Konygin et al., “Structure and magnetic properties of $\text{Fe}_{100-x}\text{Sn}_x$ ($3.2 < x < 62$) alloys obtained by mechanical milling,” *Journal of Magnetism and Magnetic Materials*, vol. 166, no. 3, pp. 334–348, 1997.
- [16] S. Takahashi and Y. Umakoshi, “Superlattice dislocations and magnetic transition in Fe-Al alloys with the B2-type ordered structure,” *Journal of Physics: Condensed Matter*, vol. 3, no. 31, pp. 5805–5816, 1991.
- [17] J. W. Cable, L. David, and R. Parra, “Neutron study of local environment effects and magnetic clustering in $\text{Fe}_{0.7}\text{Al}_{0.3}$,” *Physical Review B: Condensed Matter and Materials Physics*, vol. 16, no. 3, pp. 1132–1137, 1977.
- [18] G. P. Huffman, “Mössbauer study and molecular field theory of the magnetic properties of Fe-Al alloys,” *Journal of Applied Physics*, vol. 42, no. 4, pp. 1606–1607, 1971.
- [19] I. Vincze and A. T. Aldred, “Mössbauer measurements in iron-base alloys with nontransition elements,” *Physical Review B: Condensed Matter and Materials Physics*, vol. 9, no. 9, pp. 3845–3853, 1974.
- [20] A. Arrott and H. Sato, “Transitions from ferromagnetism to antiferromagnetism in iron-aluminum alloys. Experimental results,” *Physical Review A: Atomic, Molecular and Optical Physics*, vol. 114, no. 6, pp. 1420–1426, 1959.
- [21] A. K. Arzhnikov and L. V. Dobyshva, “Magnetic moment of iron atoms in Fe-Al body-centered cubic alloys as a function of the nearest environment,” *Physics of the Solid State*, vol. 50, no. 11, pp. 2095–2101, 2008.
- [22] E. P. Elskov, E. V. Voronina, A. V. Korolev, A. E. Elskova, and S. K. Godovikov, “On the magnetic structure of the ground state of ordered Fe-Al alloys,” *The Physics of Metals and Metallography*, vol. 104, no. 1, pp. 35–52, 2007.
- [23] A. Olariu, P. Bonville, F. Rullier-Albenque, D. Colson, and A. Forget, “Incommensurate spin density wave versus local magnetic inhomogeneities in $\text{Ba}(\text{Fe}_{1-x}\text{Ni}_x)_2\text{As}_2$: a ^{57}Fe Mössbauer spectral study,” *New Journal of Physics*, vol. 14, no. 5, Article ID 053044, 2012.
- [24] J. Cieślak and S. M. Dubiel, “Influence of charge-density wave parameters on ^{119}Sn Mössbauer spectra: calculations,” *Nuclear Instruments and Methods in Physics Research Section B: Beam Interactions with Materials and Atoms*, vol. 101, no. 3, pp. 295–302, 1995.
- [25] E. Fawcett, “Spin-density-wave antiferromagnetism in chromium,” *Reviews of Modern Physics*, vol. 60, no. 1, pp. 209–283, 1988.
- [26] A. Błachowski, K. Ruebenbauer, J. Zukrowski, K. Rogacki, Z. Bukowski, and J. Karpinski, “Shape of spin density wave versus temperature in AFe_2As_2 ($A = \text{Ca}, \text{Ba}, \text{Eu}$): a Mössbauer study,” *Physical Review B: Condensed Matter and Materials Physics*, vol. 83, no. 13, Article ID 134410, 2011.



Hindawi

Submit your manuscripts at
www.hindawi.com

